Koc. J. Sci. Eng., 8(2): (2025) 163-173 https://doi.org/10.34088/kojose.1642870

Kocaeli University

Kocaeli Journal of Science and Engineering

http://dergipark.org.tr/kojose

Optimum Aperture Radius of R-Band Rectangular Resonator for Use in Electromagnetic Material Characterization

Merve DURMUŞ [1], Alp Oral SALMAN [2,*]

[1] *MILTEK (Millimetre-wave, Electromagnetics and Security Technologies) Laboratory, Department of Electronics and Communication Engineering, Kocaeli University, Kocaeli, Türkiye,* ***ORCID:*** *0000-0001-7398-0247*

[2] *MILTEK (Millimetre-wave, Electromagnetics and Security Technologies) Laboratory, Department of Electronics and Communication Engineering, Kocaeli University, Kocaeli, Türkiye,* ***ORCID:*** *0000-0002-1708-6803*

Article Info

Research paper

Received : *February 19, 2025*

Accepted : *May 18, 2025*

Keywords

Aperture excitation,
Bethe's aperture theory,
Rectangular resonator,
R-band,
Q-factor,
Electromagnetic material characterization

Abstract

The most critical part of a resonator design for electromagnetic material characterization is determining the optimum excitation aperture radius of the resonator. 11 pairs of galvanized iron plates with apertures of various radii ranging from 3 mm to 13 mm, increasing in average radial steps of 1 mm, were fabricated for use as the excitation walls of the resonator. In measurements, each pair of plates with an aperture hole was attached between two waveguide adapters and a waveguide section. Then, *S*-parameters were measured using a network analyser. CST simulations for each case were also performed and compared with the measured ones which is not seen frequently in literature for a resonance structure. The nature of the excitation (under, critical, and over couplings) was discussed from the measured and simulated results. The quality factor values were calculated using S_{21} resonance curves obtained from both the measurements and the simulations for each radius. The optimum excitation aperture radius value for the R-band resonator was found to be approximately 7 mm for the chosen resonator dimensions. For this value of aperture, a maximum loaded quality factor was obtained, and the resonator was critically coupled. For validation, theoretical radius values were also calculated and compared with the measured and simulated ones. This is a reliable and new method for showing that the obtained values are consistent.

1. Introduction

In measuring the electromagnetic properties of the medium, the waveguide resonator method is a frequently used technique [1]. In this technique, the material's electromagnetic properties (the complex electric permittivity ε and the complex magnetic permeability μ) can be found precisely at a certain frequency, especially for low-loss materials with small relative dielectric and magnetic constants [2]. However, before measuring the electromagnetic properties, the excitation aperture radius must be determined accurately in the design of the resonator.

The most applied excitation technique of waveguide resonators is the excitation using an aperture [3]. The effect of aperture on a conductive wall was first investigated by Bethe [4]. In this study, the effect of the aperture on the common wall between two cavities to resonance and the electromagnetic fields of the cavity were examined. It was found that electric and magnetic fields in a cavity can be expressed by electric and magnetic dipoles which are in the centers of the apertures. Some generalized results for resonator and waveguide systems can be found in [5]. There, it is examined the field equations and the aperture radius using the waveguide fields for an aperture-excited resonator and an electrical equivalent circuit is used for a cavity system. Additional sources for the aperture excitation can also be found [6-8]. In those references, equivalent circuit solutions were made for various resonator and waveguide systems. Additionally, some excitation calculations between two resonators, the thickness of the excitation plate, and the effect of the aperture shape were investigated in [9-11].

The main aim of our work is to calculate the radius of

* Corresponding Author: oral.salman@kocaeli.edu.tr

the diaphragm used in the aperture excitation of a resonator operating in the R-Band in the most effective way and to support this calculation with experimental measurements and simulations. In the paper, the effects of aperture radius on the excitation of a resonator were investigated analytically, experimentally, and by simulations. As a contribution to the literature, simulated S_{21} curves are also considered as well as measured ones. Moreover, the correct aperture radius in the resonator was found in a simple but effective way and its accuracy is also tested using theoretical formulations. The theoretical (analytical) radius values were calculated by using Bethe's aperture theory from the obtained resonance curves here. Thus, a comparison was made between the radius values used in the measurements and the simulations with the analytical ones and the error rates were calculated. The excitation conditions which are under, critical, and over coupling, were determined according to the radius values of apertures. As a result, the optimum aperture radius value of an R-band waveguide resonator for material characterization was found.

Thus, comparing the aperture radii calculated using simulations and measurements with the radius values obtained from Bethe aperture theory has become a reliable new method that can be used to show whether the obtained values are consistent.

The structure of the paper is the following. The theory of the aperture excitation for a two-port cavity system is described briefly and the quality factor equations for transmission-line type calculations are shown in the first part. Necessary descriptions and results of the measurements and simulations were given in the second part. The results are handled in general terms and some recommendations are suggested for further studies in the last part.

2. Material and Methods:

2.1. Theoretical Background

To obtain radiated fields by an aperture whose linear dimensions are relatively small compared to the wavelength, there is an approximate theory (Bethe's aperture theory) that accepts the aperture as electric and magnetic dipole irradiation [4]. The magnetic and electric dipoles, which are aperture equivalents, are proportional to the normal electric field and the vertical magnetic field of the incoming wave. The aperture excitation is a frequently used method in the excitation of resonators using a rectangular waveguide. Based on the rectangular waveguide fields, resonance modes may occur because of the aperture in the resonator and the resonator can be excited in a desired mode and frequency [5]. There are three types of coupling conditions, which are under, critical, and over-coupling in the excitation of resonators. The type of excitation is determined according to the application of resonators. The appropriate coupling type for a resonator to be used in material characterization is the critical coupling. In the case of a critical coupling, at the resonance frequency, a resonator matches its load, so there is no reflection between the load and the resonator [3], and the maximum loaded quality factor of the resonator can be obtained.

2.2. Excitation of Two-Port Cavity System with Aperture

When an electromagnetic field is applied to one side of the aperture in a conductive wall, electric and magnetic dipoles will occur at the center of the aperture as described in Bethe's aperture theory [4]. If the waveguides shown in Figure 1 (a) are excited from port 1 in the dominant TE_{10} mode, a magnetic dipole occurs in the input aperture [5]. The magnetic dipole formed in this aperture generates a TE_{101} mode electromagnetic field inside the resonator. The resonator fields generate a magnetic dipole also at the output aperture to transfer the electromagnetic field in TE_{10} mode to the output waveguide (to port 2). The field equations in the resonator and output waveguide are proportional to the magnetic dipoles formed, while the magnetic dipoles are proportional to the magnetic polarizability of the aperture. The magnetic polarizability of an aperture varies according to the geometry and radius of the aperture, and it is given for a circular aperture, depending on radius as

$$\alpha_m = \frac{4}{3} r^3 \tag{1}$$

where r is the aperture radius.

The equivalent circuit for the resonator system is shown in Figure 1 (b). In this equivalent circuit, the *B* admittances, the transformers, and the *L-C-R* circuit represent the port impedances, the apertures, and the resonator, respectively. The admittance equations (not given here) can be obtained from the reflection and transmission coefficients between the guides and the resonator [5]. The extended quality factor Q_{ex} of the resonator can be obtained from these equations. The relation between Q_{ex} and magnetic polarizability α_m is given as

$$Q_{ex} = \frac{a^2 c b^2 c}{8 \alpha_m^2 \beta_{10}} \times \left(\frac{k_{101} c_0}{\pi}\right)^2 \quad . \tag{2}$$

where *a* and *b* are the standard waveguide dimensions and *c* is the resonator length. β_{10} and k_{101} are the propagation constant and the resonance wave number of the modes TE_{10} and TE_{101}, respectively. c_0 is the velocity of light in the vacuum. The derivation details of this equation can also be found in [5]. The radius of the aperture can be obtained by substituting α_m from (1) into (2) as

$$r = \left\{ \frac{9}{128} \frac{a^2 b^2 c}{Q_{ex} \beta_{10}} \times \left(\frac{k_{101} c_0}{\pi} \right)^2 \right\}^{1/6} \quad . \quad (3)$$

k_{101} and β_{10} are respectively defined as

$$k_{101} = \sqrt{\left(\frac{\pi}{b}\right)^2 + \left(\frac{\pi}{c}\right)^2} \quad , \quad (4)$$

$$\beta_{10} = \sqrt{k_{101}^2 - k_{c10}^2} \quad (5)$$

where k_{c10} is the cutoff wave number of the mode TE_{10} for waveguides and equals to $\frac{\pi}{a}$ [3].

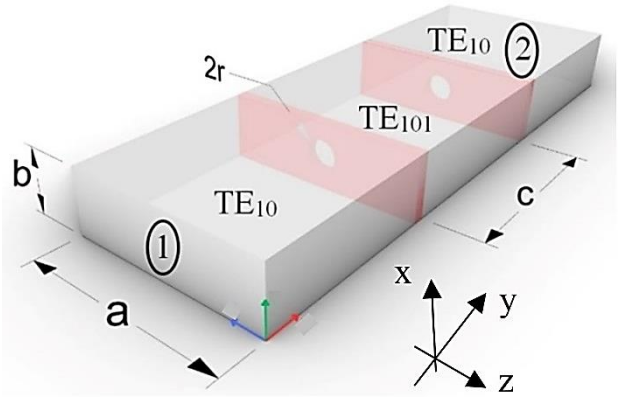

(a)

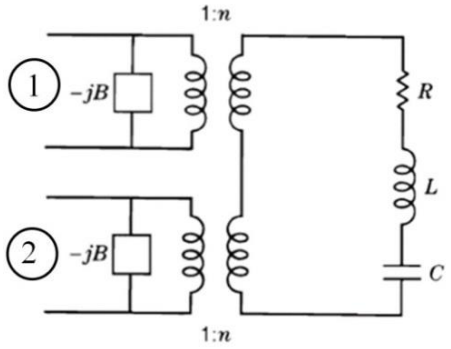

(b)

Figure 1. (a) A two-port cavity system, and (b) its equivalent circuit [5].

The resonance frequency of a rectangular resonator given in Figure 1a can be written as

$$f_r = \frac{c}{2\pi\sqrt{\mu_r \varepsilon_r}} \sqrt{\left(\frac{\pi}{b}\right)^2 + \left(\frac{\pi}{c}\right)^2} \quad . \quad (6)$$

The guide wavelength of the wave traveling in the waveguide is given as follows

$$\lambda_g = \frac{2\pi}{\beta_{10}} \quad . \quad (7)$$

The external quality factor Q_{ex} of a resonator (given in (2)) with aperture excitation for a two-port system can be found using loaded and unloaded quality factors which are referred as Q_L and Q_0.

The scattering parameter curves of a two-port system can provide the necessary data to Q_L and Q_0. Using the measured or simulated S_{21} resonance curve, Q_L is calculated by

$$Q_L = \frac{f_r}{BW_{3dB}} \quad (8)$$

where f_r is the resonance frequency, BW_{3dB} is the bandwidth of the resonance curve at -3 dB [12]. The unloaded quality factor Q_0 can be found as

$$Q_0 = \frac{Q_L}{1 - |S_{21}|_{max}} \quad (9)$$

where $|S_{21}|_{max}$ is the absolute value of the resonance curve amplitude. The relation between all quality factors for the two-port resonator system is defined as

$$\frac{1}{Q_L} = \frac{1}{Q_0} + \frac{1}{Q_{ex}} \quad . \quad (10)$$

Thus, Q_{ex} can be easily calculated using (10). Some details about quality factor measurements with analyzers can be found in [13] and [14].

As explained at the end of Section 1, three types of resonance are defined as under, critical, and over-coupling [3]. In the under-coupling region, the resonance is of low amplitude and low-quality factor Q_L due to insufficient electromagnetic power entering the resonator through the aperture. When the load and the resonator's impedances are matched, the critically coupled resonance occurs and the highest Q_L is obtained. This type of resonance is required for a resonator used in the material's electromagnetic characterization due to its high sensitivity. Although the resonance level is high in the over-coupling region, the resonance curve starts to broaden due to excess electromagnetic power entering the resonator through the aperture and it causes a decrease in Q_L value.

The electromagnetic properties of a material can be found using the resonator technique. Especially relative complex electric permittivity ε_r and relative complex magnetic permeability μ_r of a material are obtained using a resonator, where $\varepsilon_r = \varepsilon/\varepsilon_0$, $\mu_r = \mu/\mu_0$ and $\varepsilon_0 = 10^{-9}/36\pi$ F/m, $\mu_0 = 4\pi \times 10^{-7}$ H/m are permeability and permittivity of vacuum, respectively. These parameters are defined in order as

$$\varepsilon_r = \varepsilon_r' - j\varepsilon_r'' \quad \text{[F/m]} \quad (11)$$

$$\mu_r = \mu_r' - j\mu_r'' \quad \text{[H/m]} \quad (12)$$

where the real parts refer to stored electric/magnetic energies and the imaginary parts refer electric/magnetic losses. The real and imaginary parts of ε_r can be obtained using the following equations

$$\left(\frac{f_r - f_0}{f_r}\right) = A(\varepsilon_r' - 1)\frac{V_s}{V_0} \quad (13)$$

$$\frac{1}{Q_L} - \frac{1}{Q_{L,0}} = B\varepsilon_r'' \frac{V_s}{V_0} \quad (14)$$

where f_0 and f are the resonance frequencies of the empty and perturbed (with material) resonator respectively, similarly V_0 and V_s are the volumes, $Q_{L,0}$ and Q_L are the loaded quality factors. A and B are constants that depend on the configuration of the cavity and the mode of operation.

The same equations can be used by replacing ε_r's with μ_r's. The derivation details of these equations can be found in [1, 3, 15, and 16].

2.3. Measurements and Simulations

The formulation of the aperture excitation is given in the first part of the article. In this part, the optimum aperture radius for an R-band waveguide resonator is going to be found using measured and simulated values. Additionally, they are going to be compared with the calculated theoretical values from Bethe's aperture theory.

For the measurements, an air-filled ($\mu_r = \varepsilon_r = 1$) R-band resonator with dimensions a x b x c = 10.92 x 5.46 x 7.90 cm was designed, and the necessary parts were purchased (except excitation walls). The resonance frequency of the empty resonator is calculated as 2343.51 MHz using (6). For the excitation of the resonator, 11 pieces of galvanized iron plates with circular holes of different radii were machined in a workshop. Those plate pairs were used as the excitation side walls of the resonator. The radius values of the drilled holes were 3 mm, 4 mm, 5 mm, 6 mm, 7 mm, 9 mm, 10 mm, 11 mm, 12.5 mm, and 13 mm (Figure 2). The reason why galvanized plates are used as a material is to prevent corrosion and rust that may occur in the future, and their good conductivity, which is a necessary feature for the resonator walls.

To determine the optimum excitation aperture radius of the designed and implemented R-band rectangular resonator, S-parameter measurements were made with each of 11 pairs of plates with different circular aperture radii as side walls of the resonator shown in Figure 2 using a network analyzer. Those results are also going to be compared with the values obtained from CST simulations. To obtain the optimum radius, measured and simulated *S*-parameters, and quality factors of the resonances were used.

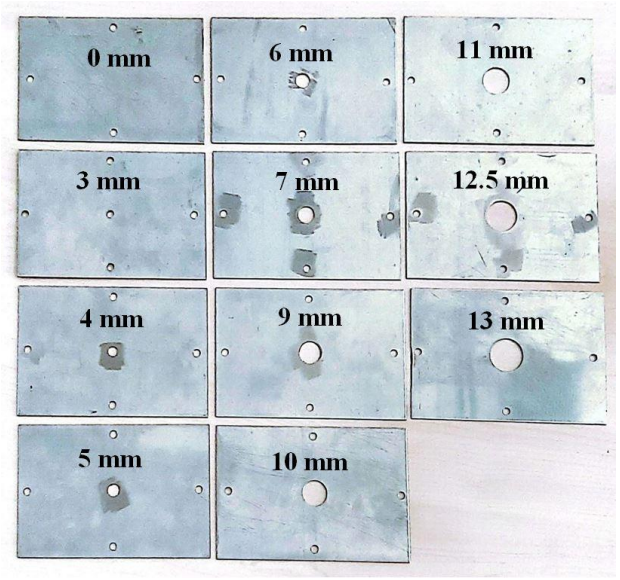

Figure 2. The machined excitation side walls with aperture holes in different radii (r = 0 mm (no hole), 3 mm, 4 mm, 5 mm, 6 mm, 7 mm, 9 mm, 10 mm, 11 mm, 12.5 mm, and 13 mm).

The R-band resonator used in the measurements (Figure 3a is composed of side walls with holes in different radii (1a, b), two coax-to-waveguide adapters (2a, b), a 7.9 cm-long waveguide piece (3), and montage screws (4). S-parameter measurements were performed using an entire R-band resonator with excitation holes of different radii with a ZVB-20 model Rohde & Schwarz network analyzer (NA) (Figure 3b). A measured resonance signal can also be seen in the photo. The "TOSM" (Through, Open, Short, Match) calibration was applied to the NA by connecting in turn each of these standards to the ends of the cables connected to two ports of the NA and calibrating them. Such calibration is necessary to compensate for possible lifetime deterioration effects of the NA and wires and to measure correct values. S_{11} and S_{21} values in the 2100-2600 MHz frequency range were measured.

CST simulations were also done to compare measured S-parameters. The simulation model used is given in Figure 4. All simulations were realized in the time domain. In the CST model, instead of drawing coax-to-waveguide adapters, which are more difficult to construct, for simplicity, 2 waveguide segments with waveguide excitation, each with a length of 2 guide wavelengths, were used (calculated from (7), $\ell = 2\lambda_g = 28.3$ cm at the central frequency of R-band waveguide 2.15 GHz);

3. Results and Discussion

Figure 5a and b give the measured and simulated S_{11} and S_{21} resonance curves versus frequency, respectively. To better highlight the details, only the ~2300-2350 MHz range

of the graph with all resonance curves has been considered. The measured S-parameter curves of the pair plates that haven't holes ($r = 0$ mm) are not shown in the figure but S-parameter levels are averagely $S_{11} \cong 0$ dB and $S_{21} \cong -100$ dB (this value can be approximately considered as the dynamic range of NA.). Similarly, the simulated values are $S_{11} \cong 0$ dB and $S_{21} \cong -200$ dB. To obtain additional data, simulations were also carried out for unmeasured apertures with 8 mm and 12 mm radii.

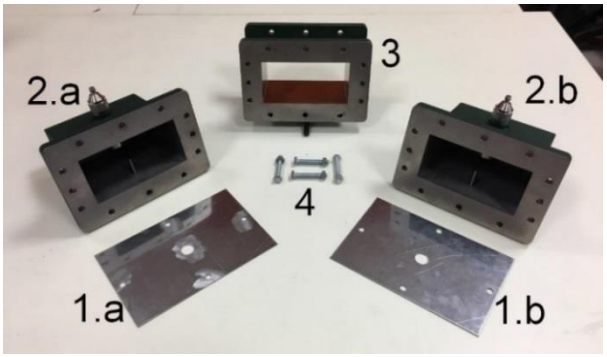

(a)

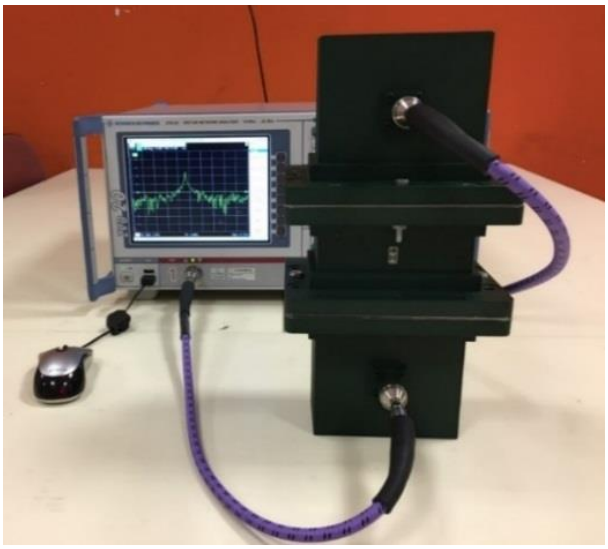

(b)

Figure 3. a) The parts of the R-band resonator used in the measurements, where 1a, 1b are the side walls with aperture holes, 2a, and 2b are the coax-to-waveguide adapters, 3 is a 7.9 cm-long waveguide piece and 4 is the montage screws. b) The combined resonator is connected to the network analyzer (NA) for measurements. A measured resonance signal can also be seen on the screen of the NA.

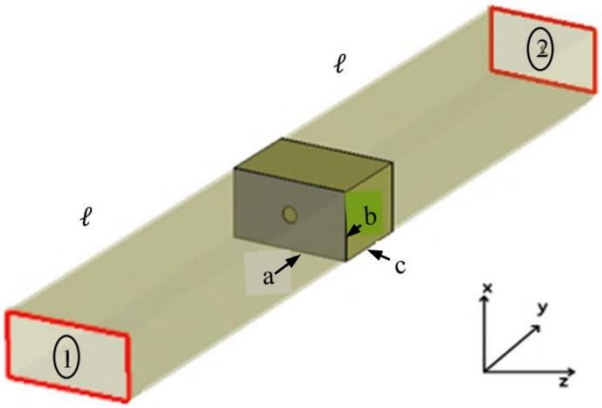

Figure 4. The applied CST simulation model is composed of two $\ell = 2\lambda_g$-long (at the central frequency 2.15 GHz) waveguide pieces and an R-band resonator with two excitation aperture holes.

As seen in Figure 5, the amplitudes of the S_{21} curves for the apertures with radii of 3 mm and 4 mm are too low due to under-coupling (low power entrance to the resonator), so they are lost in the network analyzer's noisy signal, which is around -80 dB. Resonance behavior starts to be distinguished after the 4 mm radius. For the S_{21} curves, it is seen that as the radius value increases, the resonance frequency shifts to the left towards the lower frequencies. It is also observed that when the radius value increases, the loaded quality factor Q_L values decrease due to the widening of S_{21} curves. For the aperture radius values of 9 mm and above, the type of coupling turns from under-coupling to over-coupling, because S_{11} amplitudes start to decrease faster while S_{21} levels increase and approach 0 dB in the simulation. It is an undesired case for a resonator because over-coupling causes a decrease in the quality factor Q_L. Two simulations for apertures with radii of 8 mm and 12 mm were also added in Figure 5b for extra evaluation, although they are absent in Figure 5a (not measured). The resonance frequencies in the simulations are slightly higher than the ones in the measurements. The S_{11} curves obtained from the simulations were observed to have higher amplitude values than the curves obtained from the measurements.

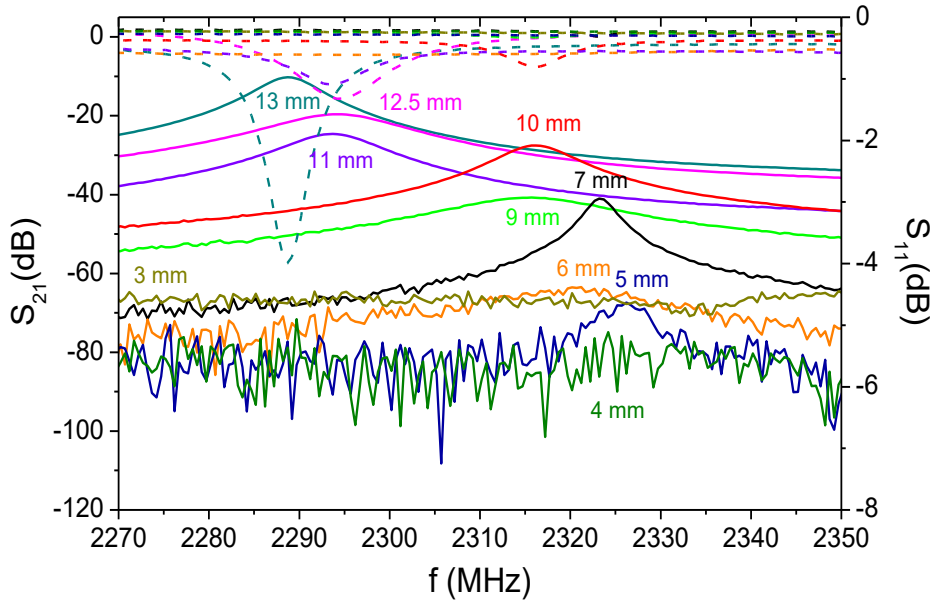

(a)

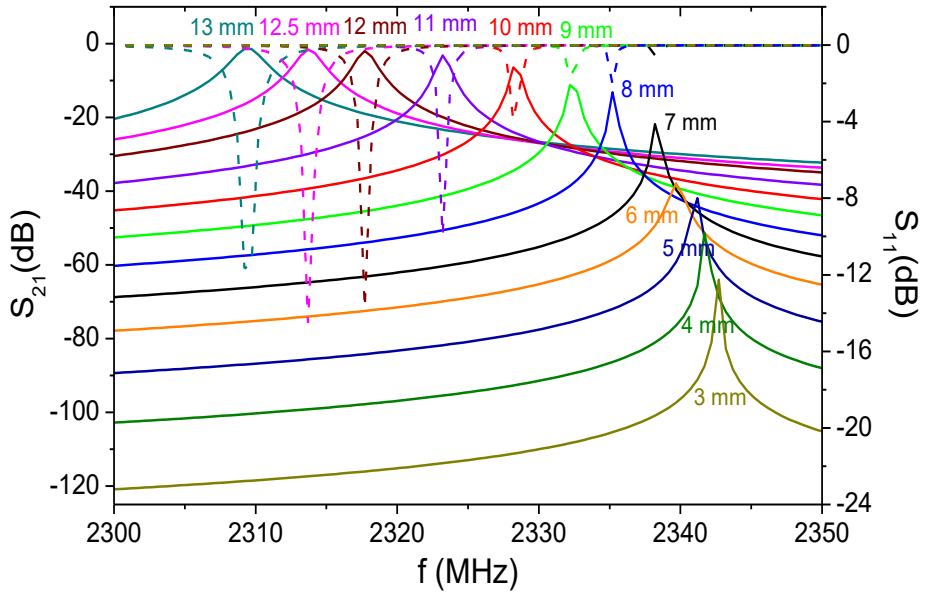

(b)

Figure 5. a) The measured and b) the simulated S_{11} (---- dashed lines), and S_{21} (—— solid lines) curves for each aperture radius *r*.

Both the measured and the simulated S_{11} and S_{21} curves are given separately for each radius in Figure 6. When the graphs are examined, it can be seen that the peaks of the resonance curves (S_{21}) are low for 5 mm and 6 mm (approx. -70 dB in the measurement, -40 dB in the simulation), and it is moderate for 7 mm (approx. -40 dB in the measurement, -20 dB in the simulation) and it is high for the other radii (approximately vary -30 dB to -10 dB in the measurements, -11 dB to -1 dB in the simulation). This situation shows that there is an under-coupling for 5 mm and 6 mm, a critical coupling for 7 mm, and an over-coupling for other larger radii.

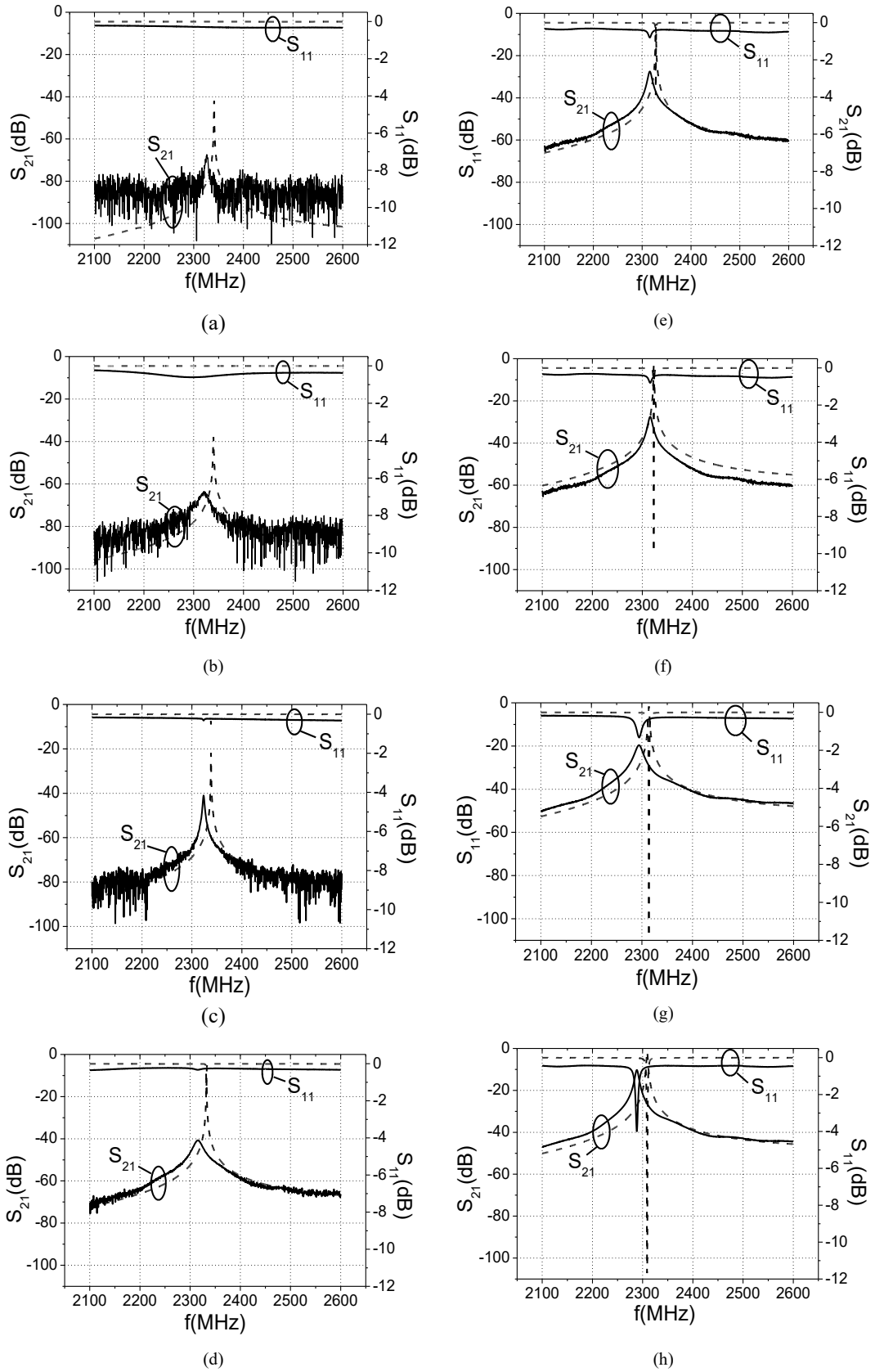

Figure 6. The measured (—) and simulated (---) S_{11} and S_{21} (resonance) curves for radii of, a) 5 mm, b) 6 mm, c) 7 mm, d) 9 mm, e) 10 mm, f) 11 mm, g) 12,5 mm, and h) 13 mm.

The measured and simulated S_{21} resonance curves were used in the calculation of quality factor values explained in Section 2.2. A MATLAB code was created for the calculations of the necessary formulas given in the theoretical part. First, for each radius, the loaded quality factor Q_L was calculated using (8). The Q_L values and the absolute values of S_{21} ($|S_{21}|_{max}$) were used to find the unloaded quality factor Q_0 values, using (9). Q_L and Q_0 values were inserted in (10) to obtain the extended quality factor Q_{ex} values for each radius. For each radius, all quality factors (Q_0, Q_L, and Q_{ex}) from measured and simulated results were calculated and tabulated in Table 1 [17].

Table 1. Quality factor values calculated from measurement and simulation results.

r (mm)	Q_L		Q_0		Q_{ex}	
	Measured	Simulated	Measured	Simulated	Measured	Simulated
5.0	581.50	4682	581.80	4720	582230.0	1359900
6.0	221.07	2924	221.22	2962	329650.0	228420
7.0	663.78	7793	669.72	8482	74673.0	95919
8.0	-	5837	-	7469	-	26725
9.0	149.40	2915	150.78	4022	16290.0	10590
10.0	289.47	2586	302.19	4941	6878.5	5428
11.0	229.33	2323	243.70	7635	3889.6	3338
12.0	-	1782	-	8864	-	2231
12.5	163.87	1156	182.98	6928	1568.6	1388
13.0	326.90	923	472.51	5948	1060.8	1093

Only Q_L values are enough to determine the optimum aperture radius in the evaluation. Q_{ex} values will be used to obtain theoretical radius values for validation purposes, as explained in Section 2.2, because the radius r term is included in (2). As seen in the table, Q_L and Q_0 values are very close to each other for small radius values, but after 10 mm radius, the difference increases linearly with the radius. Accordingly, Q_{ex} starts from very high values at small radii and decreases rapidly as the radius increases (see formulas (8), (9) and (10)).

Because Q_L variation is enough to determine the optimum aperture, only the measured and simulated loaded quality factor Q_L values versus aperture radii are shown in Figure 7 (Q_0 and Q_{ex} are not shown). A spline connection type was selected between data points for a smoother curve in the graph. Not to forget that a resonator to be used in the electromagnetic material characterization must have a high sensitivity. To achieve this, a high-valued loaded quality factor Q_L must be chosen. According to the measurement and the simulation results, the highest value of Q_L is found at around 7 mm radius which is 663.78 for measurement and 7793 for simulation, respectively. Simulated values are approximately ten times larger than measured values. The reason for the large difference between the measured and the simulated results is the analysis method that was chosen. If the frequency domain analysis was preferred instead of the time domain analysis as the analysis method in CST, the difference between simulated and measured values could decrease from approximately ten times to two to four times depending on the aperture radius values.

The graph can be divided into three regions. The first one is the under-coupling region where there are 5- and 6-mm radius apertures. The loaded quality factor Q_L values are moderate-leveled in this region. A critical coupling phenomenon is observed at a 7 mm radius after this region (maximum measured and simulated Q_L values). Then both measured and simulated loaded quality factors start to decrease very fast in the over-coupling region (between 8 – 13 mm aperture radii).

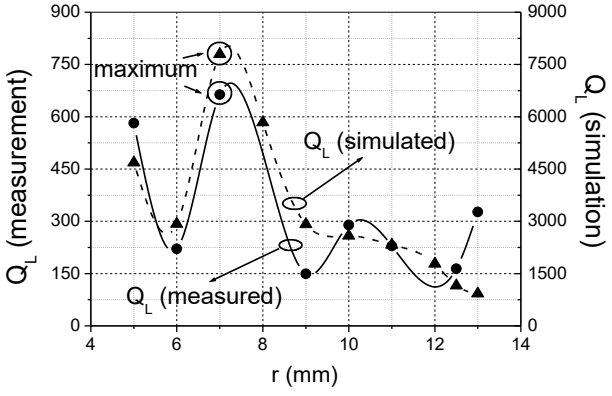

Figure 7. The measured (—●—) and simulated (--▲--) Q_L loaded quality factor values versus aperture radii.

From the loaded quality Q_L graphs given in Figure 7, one can see that a 7 mm radius is the correct choice because it has the maximum value for the best material characterization sensitivity. According to the electrical permittivity and magnetic permeability equations for the resonator ((13) and (14)), the cavity and perturbed (with material) resonance frequencies may be very close for materials with low dielectric permittivity. Therefore, to separate close resonances, the loaded quality factor Q_L of the resonance must be the highest which gives a good sensitivity.

This is the only criterion for precise measurements in the electromagnetic characterization of materials (selection of the maximum Q_L value). A more precise aperture value could be found with a set where the aperture radius varies in smaller steps (e.g. 0.5 mm intervals).

The validation of the aperture radius r values can be done by comparing the theoretical (analytical) radius values obtained from (3) with the ones obtained from the Q_L value calculated using measured and simulated S_{21} curves. The procedure is explained in the following. From the measured and simulated loaded quality factors Q_L and unloaded quality factors Q_0 are calculated using (8) and (9), respectively. Then both Q_L and Q_0 are inserted into (10) to obtain extended quality factor Q_{ex} values. Those Q_{ex} values are inserted into (3) to find the radius. The theoretical (analytical) radius for measured and simulated values and error rates was calculated for all aperture radii and tabulated in Table 2. It can be seen from the table that the theoretical values calculated using the measured and simulated quality factors for the 7 mm radius where the critical coupling occurs are 6.8 mm and 6.6 mm, respectively, and these values are quite close to the obtained value of 7 mm with a percentage error rates are 2.86% and 5.71% respectively. The theoretical values calculated for the other aperture radii have been found using the same method and the error rates vary between 2 % to 16 % and 2 % to % 6.4 for measured and simulated values, respectively.

Remember the calculated resonance frequency for the chosen dimensions of the resonator using (6), which is $f_r = 2343.51$ MHz. In Figure 8, the variations of resonance frequencies and amplitudes of resonance curves with aperture radius are shown. One can see from Figure 8a, that the resonance frequencies range from 2288.3 MHz for 13 mm to 2326.2 MHz for 5 mm in the measurements and they are in the interval 2309 MHz – 2341 MHz in the simulations. As the radius value increases, the resonance frequency decreases. This is observed in both measurement and simulation results. As the radius r value decreases, the measured and simulated resonance frequency values approach the theoretical resonance frequency value calculated from (6). From Figure 8b, one can see that the larger the diameter, the more power enters the resonator (this causes a larger resonance magnitude $|S_{21}|_{max}$ value).

Table 2. Calculated theoretical (analytical) radius values using measured and simulated values for comparison, and the error rates for them.

r (mm)	$r_{theoretical}$ (mm)		% Error	
	From Measured Values	From Simulated Values	From Measured Values	From Simulated Values
5.00	4.2	4.9	16.00	2.00
6.00	5.3	5.7	11.67	5.00
7.00	6.8	6.6	2.86	5.71
8.00	-	8.1	-	1.25
9.00	8.8	9.5	2.23	5.56
10.00	10.2	10.6	2.00	6.00
11.00	11.2	11.5	1.82	4.55
12.00	-	12.3	-	2.50
12.50	13.0	13.3	4.00	6.40
13.00	13.9	13.8	6.92	6.15

4. Conclusions

An R-band resonator to be used in the electromagnetic characterization of materials has been designed and realized. The most important parameter in the design was to determine the optimum radius of the excitation aperture obtained for these resonator dimensions. The maximum loaded quality factor Q_L value in the critical coupling region is the main criterion to find the optimum aperture radius value. This optimum aperture radius was found as approximately 7 mm for the chosen dimensions of the resonator by applying this criterion. For comparison, theoretical aperture radius values using the measured and the simulated Q_{ex} values were also found using Bethe's aperture theory (3) with the procedure explained in the text, and quite close values to the real aperture radius were obtained. This shows that the correct procedure was applied to find the optimum aperture value.

Thus, two points can be stated as contributions to the literature: 1) The accuracy of the experimental measurements was ensured by using simulated curves in addition to the measurements, 2) The theoretical aperture radius values in Bethe aperture theory were compared with the values calculated from measurements and simulations, and this was shown to be an important tool that can be used in verifying the obtained results.

A more precise aperture value could be found with a set where the aperture radii change in smaller steps. The same methodology can be applied to find the optimum

aperture radius for the rectangular resonators operating in other bands.

With this method proposed for finding the optimum aperture radius of a rectangular resonator, the aperture radii of resonators operating in other bands (such as L, S, C and other bands) can be found most effectively.

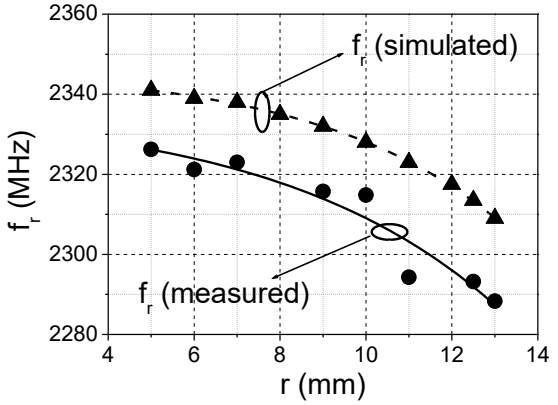

(a)

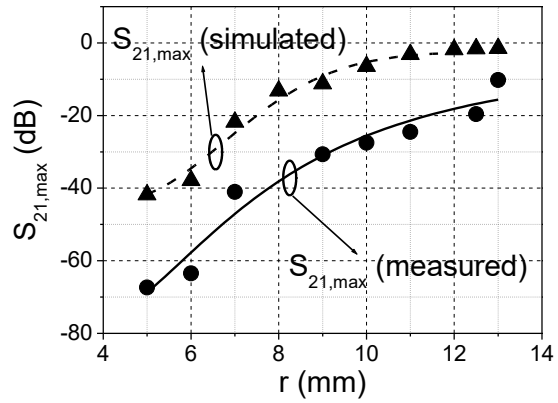

(b)

Figure 8. a) The resonance frequencies and b) S_{21} resonance amplitudes, versus radius, for measured (——) ● and simulated (------) ▲ results.

Declaration of Ethical Standards

The authors of this article declare that the materials and methods used in this study do not require ethical committee permission and/or legal-special permission.

Conflict of Interest

The authors declare that they have no known competing financial interests or personal relationships that could have appeared to influence the work reported in this paper.

References

[1] Chen L.F., Ong C.K., Neo C.P., Varadan V.V., Varadan V.K., 2004. Microwave Electronics: Measurement and Materials Characterization, West Sussex: John Wiley & Sons, England.

[2] Vinoy K.J., Jha R.M., 1996. Radar Absorbing Materials: From Theory to Design and Characterization, Boston: Kluwer Academic Publishers, USA.

[3] Pozar D.M., 2012. Microwave Engineering, 4th ed. New Jersey: John Wiley & Sons Inc., USA.

[4] Bethe H.A, 1944. Theory of Diffraction by Small Holes. Physics Review, **66**, pp. 163-182.

[5] Collin R.E., 1990. Field Theory of Guided Waves., 2nd ed., John Wiley & Sons Ltd., New York, USA.

[6] Stratton J.A., 1941. Electromagnetic Theory. McGraw-Hill Book Co., New York, USA.

[7] Montgomery C.G., 1948. Principles of Microwave Circuits, McGraw-Hill Book Co. Inc., New York, USA.

[8] Marcuvitz N., 1951. Waveguide Handbook., McGraw-Hill Book Co. Inc., New York, USA.

[9] McDonald N.A., 1972. Electric and Magnetic Coupling through Small Apertures in Shield Walls of any Thickness. IEEE Transactions on Microwave Theory and Techniques, **20**, pp. 689-695.

[10] McDonald N.A., 1985. Polynomial Approximations for the Electric Polarizabilities of Some Small Apertures. IEEE Transactions on Microwave Theory and Techniques, **33**, pp.1146-1149.

[11] Wheeler H.A., 1964. Coupling Holes Between Resonant Cavities or Waveguides Evaluated in Terms of Volume Ratios. IEEE Transactions on Microwave Theory and Technique, **12**, pp. 231-244.

[12] Kajfez D., Chebolu S., Abdul-Gaffoor M.R., Kishk A.A., 1999. Uncertainty Analysis of the Transmission Type Measurement of Q-Factor. IEEE Transactions on Microwave Theory and Techniques, **47**, pp. 367-371.

[13] Kajfez D., Hwan E.J., 1984. Q Factor Measurements with Network Analyzer. IEEE Transactions on Microwave Theory and Techniques, **32**, pp.666-670.

[14] Kajfez D., 1995. Q Factor Measurements with Scalar Network Analyzer. IEE Proc.-Microw. Antennas Propag., **142**, pp. 369-372.

[15] Sucher M., Fox J., 1963. Handbook of Microwave Measurements, 3rd ed., John Wiley and Sons, West Sussex, England.

[16] Salman A.O., Alper F. 2023, R-Bant Boşluk Rezonatörü ile Bazı Mikrodalga Malzemelerinin Karmaşık Dielektrik ve Manyetik Geçirgenliklerinin Belirlenmesi. Kocaeli Üniversitesi Fen Bilimleri Dergisi, **6**, pp. 27-35.

[17] Durmuş M., 2018. R-Bant Dikdörtgen Boşluk Rezonatörü için Uygun Uyarım Açıklık Yarıçapının Bulunması. M.Sc. Thesis. Kocaeli Universitesi Fen Bilimleri Enstitüsü.